THE JOURNAL OF PHYSICAL CHEMISTRY B

Article

pubs.acs.org/JPCB

# Quantum-Chemical and Molecular Dynamics Study of $M^+[TOTO]^-$ (M = Li, Na, K) Ionic Liquids

Andrzej Eilmes* and Piotr Kubisiak

Faculty of Chemistry, Jagiellonian University, Ingardena 3, 30-060 Kraków, Poland

Supporting Information

**ABSTRACT:** Quantum-chemical calculations and classical molecular dynamics simulations with the Optimized Potentials for Liquid Simulations-All Atom (OPLS-AA) force field are presented for ionic liquids based on 2,5,8,11-tetraoxatridecan-13-oate anion (TOTO) and alkali cations (Li, Na, K). Complexation energies decrease with increasing cation radius from Li to K. Cation interactions with carboxylate oxygen atoms are preferred over complexation to ether oxygens. Cross-linking occurs in the structure of the liquid because of interactions of multiple metal ions with carboxylate oxygen atoms from multiple TOTO anions. Anticorrelated motion of ions of the same charge is an important factor decreasing conductivity of the liquid. Results of modeling agree with available experimental data for Na-TOTO.

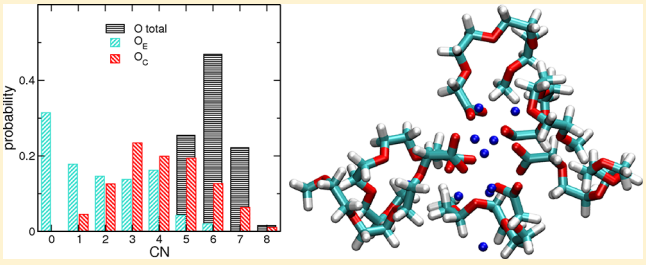


## 1. INTRODUCTION

Room-temperature ionic liquids (RTILs) are organic salts which are in liquid state at ambient temperatures. Such liquids are receiving considerable attention because of the range of their potential applications as alternative solvents and reaction media in synthesis and catalysis, as electrolytes in fuel cells and batteries, as media in separation technology, and so forth.[1,2] Their advantages are nonflammability, very low vapor pressure, possibility of recycling, making ionic liquids promising candidates to replace traditional volatile organic solvents in industry.[3] Therefore, ILs are well in the focus of green chemistry research.

A huge variety of possible anion−cation combinations which may be used in ionic liquids opens the possibility of designing tunable solvents, tailored for specific applications, by an appropriate choice of anion−cation pair. A large amount of experimental and theoretical effort is therefore invested in optimizing properties of ILs for particular purposes. Research on ionic liquids concentrates mainly on imidazolium, pyridinium, or pyrolidinium derivatives. However, several other systems are investigated, including those based on simple cations.

Recently, a new class of ionic liquids with low cytotoxicity, alkali oligoether carboxylates, has been introduced and characterized in physicochemical measurements.[4−7] These systems are based on alkali cations (e.g., $Na^+$) and 2,5,8,11-tetraoxatridecan-13-oate anion ($CH_3O-(CH_2-CH_2-O)_3-CH_2COO^-$, $[TOTO]^-$). The structure of the anion resembles oligoglymes (oligoethylene glycol methyl ethers, $CH_3O-(CH_2-CH_2-O)_n-CH_3$), well-known as complexing agents for alkali cations because of the presence of oxygen atoms in the oligoether chain. $[TOTO]^-$ contains also a carboxylate group, which even more strongly interacts with metal ions. Therefore, the total interactions of alkali cations with $[TOTO]^-$ anion result from the balance of $M^+$ interactions with carboxylate or ether oxygen atoms. Depending on their relative strength, M−TOTO IL might be viewed as a liquid with a crown etherlike complex as a dominating structural feature or as a more complicated structure in which metal ions interacting with oxygen atoms from different anions act as cross-linkers between TOTO anions. Such possible scenarios have been discussed in ref 5.

Ion−ion interactions in ionic liquids have been extensively theoretically studied by a range of methods including quantum-chemical calculations and classical or ab initio molecular dynamics simulations.[8−14] Most of the theoretical works investigated typical (e.g., imidazolium-based) ILs. Except for quantum-chemical calculations performed for $Na^+[TOTO]^-$ complex,[5] no systematic theoretical modeling of oligoether carboxylates has been reported. On the other hand, metal ion interactions with oligoether oxygens have been already studied for olygogymes and poly(ethylene oxide) systems in the context of solid electrolytes. Cation complexation energies have been calculated by quantum-chemical methods,[15−20] and the structure and dynamics of the electrolyte has been investigated via molecular dynamics.[21−26]

Although one could expect some similarities between the structure and properties of salt solutions in oligoglymes and alkali ion−TOTO systems, the presence of negatively charged carboxylate groups, attracting metal cations, is likely to influence interactions in TOTO-based ILs. Therefore, in this paper, we attempted a theoretical study of M−TOTO ionic

**Received:** July 16, 2013
**Revised:** September 22, 2013
**Published:** September 25, 2013

liquids. In particular, we wanted to assess to what extent such systems resemble oligoglyme electrolytes and how large is the impact of $COO^-$ groups on interionic interactions in the liquid.

In the experiment,[4,5] only $Na^+-[TOTO]^-$ has been thoroughly investigated. Liquid with $Li^+$ cation has too large viscosity, and $K^+-[TOTO]^-$ is in solid state at room temperatures; therefore, there are no experimental data regarding conductivity of these two systems. Nevertheless, we will examine systems with three different alkali metals (Li, Na, K) to check how much the type of the cation influences interactions in the system affecting properties of the IL. We will show results of quantum-chemical calculations and classical molecular dynamics simulations and discuss how they can help to elucidate structure of the liquid and its relation to physicochemical properties.

## 2. QUANTUM-CHEMICAL CALCULATIONS

The chemical formula of M−TOTO is shown in Table S1 of the Supporting Information; the structure of the anion can also be seen in Figure 1. Gaussian 09 rev. A.02[27] was used for all quantum-chemical calculations reported in this work. Geometries of $[TOTO]^-$ and its 1:1 complex with alkali cations were optimized using Møller−Plesset method and 6-31++G** basis set. The same level of theory was used to compute stabilization energies for anion−cation complexes. In addition to vacuum calculations, we also performed computations with the polarizable continuum model (PCM) used to account for the solvent. Static dielectric permittivity was set to $\varepsilon = 22$ corresponding to the experimental value for Na−TOTO.[5] Default parameters (Universal Force Field (UFF) atomic radii and van der Waals surface) were used to build the molecular cavity. Geometry optimizations in the solvent as well as single-point energy calculations for vacuum geometries were performed using the PCM approach.

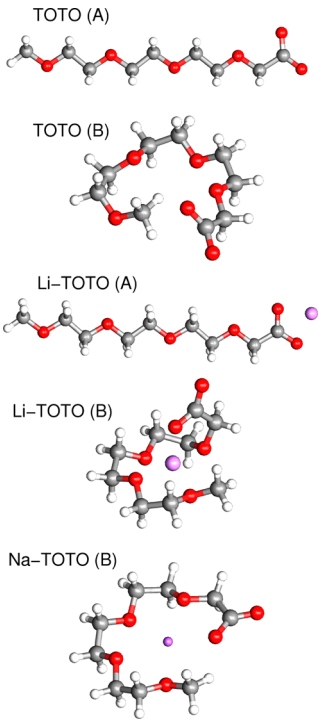


**Figure 1.** Geometries of $[TOTO]^-$ and sample $M^+-[TOTO]^-$ complexes optimized at the MP2/6-31++G** level in vacuum.

Optimal geometries resulting from the MP2/6-31++G** optimizations in vacuum are displayed in Figure 1. For isolated $[TOTO]^-$ anion, two structures corresponding to local minima of potential energy were found: all-trans chain (referred to as structure A, Figure 1) and the twisted conformation (structure B). The latter structure is about 2 kcal/mol more stable than the straight-chain conformation.

Accordingly, we found two types of $M^+-[TOTO]^-$ complexes: one with all-trans conformation of the $[TOTO]^-$ anion and the metal ion interacting with two carboxylate oxygen atoms (structure A) and the other with the anion twisted around the cation (structure B). In the latter structure, $[TOTO]^-$ anion coordinates the cation by all four ether oxygens and one oxygen atom from the carboxyl group. In Figure 1, both kinds of structures are shown for Li−TOTO. For $Na^+$ and $K^+$ ions, structure B differs from corresponding Li−TOTO geometry in the orientation of the $COO^-$ group. In Na−TOTO and K−TOTO, all oxygen atoms lie approximately in the same plane, while in Li−TOTO, a twist of the carboxylate group locates its oxygen atom above the plane of ether oxygens allowing more dense packing of oxygen atoms around the small $Li^+$ cation. Na−TOTO is shown in Figure 1 as an example; the structure of this complex is essentially the same as that found in quantum-chemical calculations in ref 5.

In Table 1, we displayed metal−oxygen distances in all structures. With the radius of the ion increasing from $Li^+$ to $K^+$, $M^+-O$ distances increase in the same sequence. For a given ion, the distance to the ether oxygen atom is always larger than the distance to the carboxylate oxygen, confirming larger interaction strength with the latter.

Complexation energy $E_c$ of metal ion $M^+$ was calculated as

$$E_c = E_{M-TOTO} - (E_{TOTO} + E_M) \quad (1)$$

where $E_{M-TOTO}$ is the energy of the $M^+-[TOTO]^-$ complex; $E_{TOTO}$ and $E_M$ stand for the energy of the $[TOTO]^-$ ion in its

**Table 1. Complexation Energies in Vacuum and in the PCM Solvent ($\varepsilon = 22$), BSSE Values in Vacuum, and $M^+-O$ Distances Calculated for $M^+-[TOTO]^-$ at the MP2/6-31++G** Level**

| system | $E_c$(vac) (kcal/mol) | BSSE(vac) (kcal/mol) | $E_c$(PCM) (kcal/mol) | $M^+-O$ distances (Å) | |
|---|---|---|---|---|---|
| | | | | $O_C$ | $O_E$[a] |
| TOTO−Li (A) | −162.3 | 2.4 | −13.1 | 1.89, 1.90 | |
| TOTO−Li (B) | −197.6 | 7.7 | −34.5 | 1.85 | 2.13, 2.06, 2.07, 2.02 |
| TOTO−Na (A) | −137.4 | 2.0 | −10.1 | 2.26, 2.26 | |
| TOTO−Na (B) | −161.1 | 6.1 | −24.3 | 2.24 | 2.38, 2.59, 2.59, 2.42 |
| TOTO−K (A) | −121.2 | 3.6 | −11.1 | 2.57, 2.57 | |
| TOTO−K (B) | −139.5 | 8.1 | −26.8 | 2.51 | 2.65, 2.82, 2.82, 2.74 |

[a] $O_E$ atoms are numbered from the $COO^-$ group of the anion toward the $CH_3$ end.


dx.doi.org/10.1021/jp4070449 | J. Phys. Chem. B 2013, 117, 12583−12592

twisted (B) conformation and the energy of an isolated metal cation, respectively. Complexation energies were calculated both in vacuum and in the PCM solvent. Resulting values are collected in Table 1. Binding energies obtained using the PCM approach for geometries optimized in the solvent and from the single-point PCM energies calculated at vacuum geometries do not differ more than 1 kcal/mol; therefore, only the latter values are displayed in Table 1. To estimate the effect of basis set incompleteness, basis set superposition error (BSSE) corrections to the complexation energy were calculated in vacuum. BSSE values are larger for structures (B) (up to 8 kcal/mol), whereas in complexes (A), they reach 2−3 kcal/mol. In vacuum calculations, BSSE values are only small corrections compared to full complexation energies.

Structures of type (B) are better stabilized than complexes (A) owing to a larger number of metal−oxygen interactions. The average stabilization energy per carboxylate oxygen atom $O_C$ in structures (A) in vacuum is about 81, 69, and 61 kcal/mol in $[TOTO]^-$ complexes with $Li^+$, $Na^+$, and $K^+$, respectively. Assuming that these values are transferable to structures of type (B) (which seems justifiable as the $M-O_C$ distances in both structures are very similar), we obtain 29, 23, and 20 kcal/mol as average stabilization in vacuum per one interaction of ether oxygen atom $O_E$ with Li, Na, or K ion, respectively. As readily seen, the strength of the cation−$[TOTO]^-$ interaction, calculated either per individual interaction with one oxygen atom or as total stabilization energy of the complex, decreases with increasing $M^+$ radius. The $Li^+-O_E$ distances in the Li−TOTO (B) structure are a little larger than the values of about 2.0 Å obtained for the $Li^+$ complex with triglyme[16,20] (i.e., in case of 4-fold coordination of the cation). Likewise, the average stabilization energy 29 kcal/mol per $Li^+-O_E$ estimated for Li−TOTO is similar to the values of 26−27 kcal/mol for the average $Li^+$ interaction with triglyme oxygen atom.[16,20] Cation interactions with ether oxygen atoms in TOTO are therefore of almost the same strength as in complexes with oligoglymes. Stabilization energies calculated in condensed phase are significantly smaller than corresponding values obtained in vacuum because of effective screening of electrostatic interactions. Depending on the cation, complexation energies in the solvent are in the range from −10 to −13 kcal/mol for structures of type (A) and between −24 and −35 kcal/mol for complexes (B).

Interactions of the cation with carboxylate oxygens in vacuum are 2.5−3 times stronger than with ether oxygen (which is not surprising as $O_C$ atoms bear more negative partial charge), and they should be preferred in the complex. In the solvent, contributions from both kinds of interactions are similar (about −5 to −7 kcal/mol per one contact). BSSE corrections are larger for structures (B); therefore, they slightly increase preference for interactions with carboxylate oxygens. Nevertheless, with a larger number of ether oxygen $O_E$ atoms available in the $[TOTO]^-$ anion, the twisted structure (B) is favorable for a single cation−anion pair over the geometry (A) because the net effect of four $M^+-O_E$ interactions compensates for the missing $M^+-O_C$ interaction. Accordingly, the twisted structure (B) with more $M^+-O$ contacts is preferred in quantum-chemical calculations for a 1:1 complex. On the other hand, in the liquid, where the alkali ion may interact with many anions, the preferable coordination pattern may be different, and one may expect that the percentage of $M^+-O_C$ contacts increases. We will attempt to verify this in molecular dynamics (MD) simulations.

## 3. MOLECULAR DYNAMICS SIMULATIONS

**3.1. Simulation Details.** All MD simulations were performed with the Optimized Potentials for Liquid Simulations (OPLS) all-atom nonpolarizable force field.[28] Parameterization of bonded parameters (bonds, angles, and dihedrals) as well as van der Waals interactions was taken from refs 28 and 29. Atomic partial charges were determined from quantum-chemical calculations (at the B3LYP/aug-cc-pvdz level) using the Merz−Kollman fit to electrostatic potential. Values of atomic charges used in simulations are collected in the Supporting Information.

As a test of the parametrization, we compared complexation energies calculated quantum-chemically in section 2 with values obtained from the force field. Calculations were performed either at fixed geometries resulting from MP2 calculations or for structures relaxed using molecular mechanics and the OPLS parametrization; the results are collected in Table S2 of the Supporting Information. Force-field values of stabilization energy are underestimated with respect to MP2 values; the difference is about 7−10 kcal/mol (depending on the cation and the geometry of the complex) and reaches a maximum value of 14 kcal/mol for K−TOTO in geometry (A). With total complexation energies between −190 and −120 kcal/mol, such accuracy is quite satisfactory.

Molecular dynamics simulations were conducted using NAMD v. 2.8 and 2.9 package.[30] Experimental conductivity data for Na−TOTO are reported for the temperature range 300−420 K.[4] At low temperatures, the dynamics of the liquid is remarkably slow: viscosity is large (in the case of Li−TOTO to the extent of preventing measurements) and conductivity is small. It is therefore expectable that in MD simulations at low temperatures systems will be close to solid state with very slow ion movements, requiring very long times to equilibrate the structure of the liquid and making it hard to obtain transport properties such as diffusion coefficients. Therefore, to make the effect larger, we decided to simulate systems close to the upper temperature limit used in experiments. All simulations were performed in the NPT ensemble at $T$ = 400 K and $p$ = 1 atm with Langevin dynamics and modified Nose-Hoover Langevin barostat used to control temperature and pressure. A time step of 1 fs was used to integrate equations of motion. Periodic boundary conditions were applied to the system, and electrostatic interactions were taken into account via particle mesh Ewald (PME) algorithm.

The speed of scientific computations can be greatly increased using general purpose graphic processing units (GP GPU) computing (supplementing or replacing standard central processing unit calculations). GPU acceleration is available in NAMD program; therefore, we attempted some performance tests on machines equipped with two Intel Xeon E5645 CPUs and eight NVidia Tesla M2090 GPUs. The system sizes tested ranged from 100 to 12 800 $M^+-[TOTO]^-$ pairs (3300−422 400 atoms). The results are collected in the Supporting Information. Generally, the benefits of GPU computing become visible for larger systems; even then, there is no gain in speed when the number of GPUs used in simulations exceeds two. Preliminary tests showed that there are no significant differences between results obtained for systems consisting of 100 or 800 ion pairs. Therefore, in production simulations, we used systems with 100 $M^+-[TOTO]^-$ pairs to reduce computational effort.


dx.doi.org/10.1021/jp4070449 | J. Phys. Chem. B 2013, 117, 12583−12592

The results of MD simulations, especially in the case of strong interactions between ions leading to possible ion entrapment, may depend on the initial structure of the system. For each cation, we used three starting geometries: (I) structure built from randomly placed complexes of type (A); (II) analogous structure composed of complexes (B); (III) structure where cations and anions were distributed completely randomly. Therefore, in structures I and II, metal ions were coordinated by carboxylate and ether oxygen atoms, respectively, whereas there was no coordination pattern in the initial structures of type III. Packmol[31] program was used to build random structures with periodic boundary conditions. About 250 ns of MD trajectory was collected for each system; further simulations (up to 500 ns total trajectory) were performed for structures III and also for some structures of type I (with Li and Na ions).

To check to what extent our systems reached equilibration in the course of MD simulations, we monitored the density of the system, the average coordination numbers, and the radial distribution functions. We have observed that these values tend to stabilize after about 300 ns.

**3.2. Structure of the M−TOTO Liquid.** After initial equilibration, the densities of the systems stabilize at about 1.16, 1.19, and 1.20 g/cm$^3$ for M = Li, Na, and K, respectively. The measured density of $Na^+$−[TOTO]$^-$ decreases linearly with temperature[32,4] and in the range of 298−338 K can be fit as a straight line with $R^2$ = 0.999999. Extrapolating this experimentally established dependence, one obtains $\rho$ = 1.20 g/cm$^3$ at 400 K; therefore, the result of our simulations agrees well with experimental data.

As a first step of the analysis of MD trajectories, we examine evolution of $M^+$ coordination numbers (CNs) defined as the number of $O_C$ or $O_E$ oxygen atoms found within the sphere of radius 3 Å (for $Li^+$ and $Na^+$) or 4 Å ($K^+$) centered at the metal ion (reasons for such choice of radii will be shown later). Data obtained for all three types of initial systems are shown in Figure 2 as the CN dependence on time. To smoothen the plots, the running average over 1 ns was applied to CN($t$) data.

Changes of CNs are the fastest for K−TOTO for which curves obtained for all three systems converge after about 250 ns. The evolution is the slowest in the case of Li−TOTO. Such a result is not surprising, because strong interactions of $Li^+$ with anions slow down cation motions and changes of the structure of the system. It is apparent that systems evolve toward structure similar to I rather than to the structure of a liquid where most cations are complexed in a chelatelike way as in II. In fact, in systems of II, significant reorganization takes place: the coordination number to $O_E$ oxygens decreases and, simultaneously, CN to $O_C$ increases.

As an additional measure of structural changes in the system, we calculated average end-to-end [TOTO]$^-$ distance $d_{EE}$, defined as the distance between the carbon atom from the terminal $CH_3$ group and the carbon atom from the carboxylate group. For isolated anions, $d_{EE}$ amounts to 14.3 Å for conformation (A) and 3.5 Å for geometry (B). The plot of $d_{EE}(t)$ changes during MD simulation is available in the Supporting Information (Figure S1). At the end of the trajectory, $d_{EE}$ for systems I and III reaches 8.5 Å (therefore, it is halfway between geometries (A) and (B)). For systems II, $d_{EE}$ increases steadily from the initial value below 6 Å, showing that TOTO anions which were initially wrapped around counterions start to unwrap. This allows cations to change their coordination. All these parameters indicate that, as suggested by the relative strength of different cation−oxygen interactions, $M^+$−$O_C$ contacts are preferred in the structure of M−TOTO liquid.

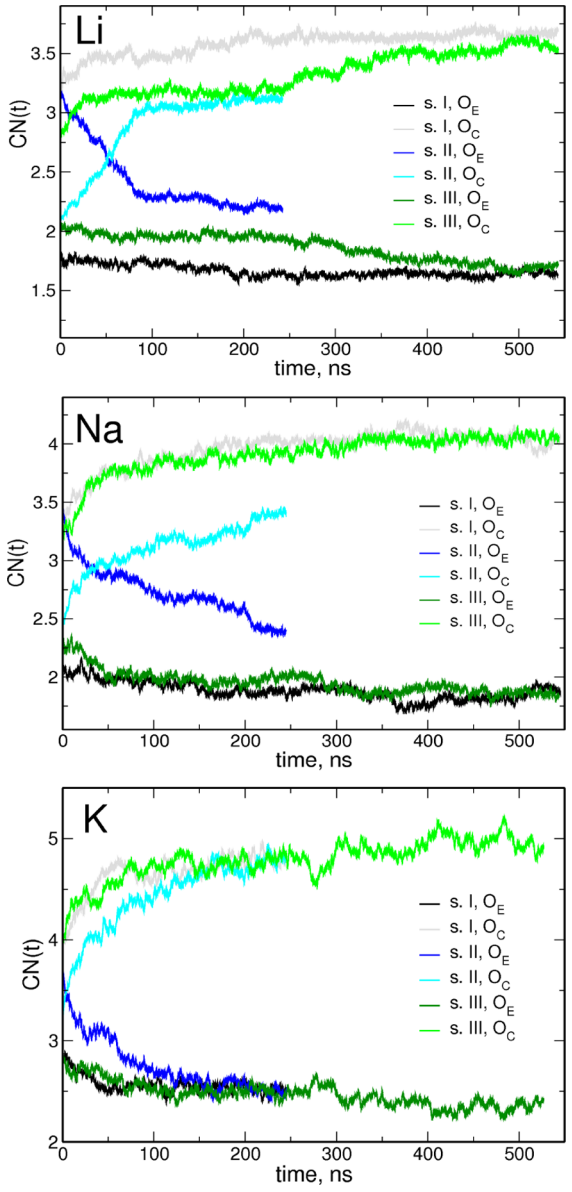


**Figure 2.** Changes in the average coordination numbers of metal ions to carboxylate ($O_C$) and ether ($O_E$) oxygen atoms along MD trajectories for three different initial structures. The curves are the running averages of CN($t$) over 1 ns.

It can be seen that systems I and III behave similarly during MD simulations; therefore, in further analysis in the main paper we will focus on systems III as they do not impose any particular structure owing to their random initial geometries. Additional analysis for structures I is available in the Supporting Information.

To obtain some information about metal−oxygen distances, we analyzed radial distribution functions (RDF) for M−O pairs. In Figure 3, RDFs are plotted for all three cations at 400 K. Total RDFs as well as RDFs separated for M−$O_C$ and M−$O_E$ are presented. As seen in Figure 3, positions of the maxima obtained for both types of oxygen atoms coincide, and they are located roughly at the M−$O_E$ distance calculated quantum-chemically. The most probable $M^+$−O distances are therefore


dx.doi.org/10.1021/jp4070449 | J. Phys. Chem. B 2013, 117, 12583−12592

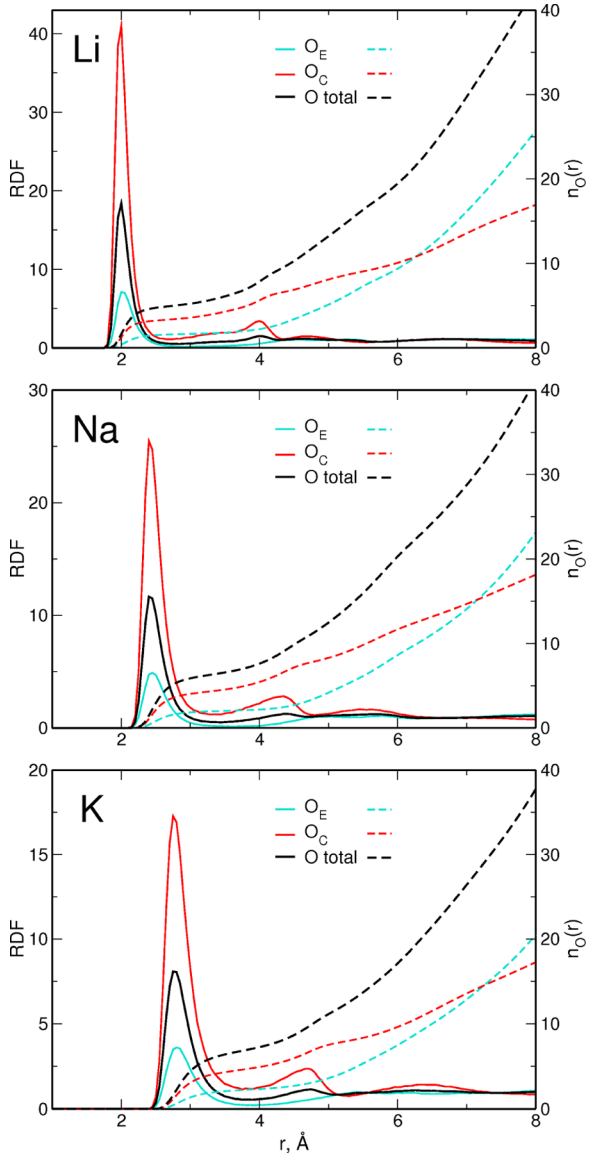


**Figure 3.** Radial distribution functions and distance-dependent coordination numbers $n(r)$ for $M^+$–O pairs.

about 2, 2.4, and 2.8 Å for M = Li, Na, and K, respectively. This peak in RDF is the sharpest for $Li^+$ and becomes lower for $Na^+$ and $K^+$. The RDF maximum corresponding to carboxylate oxygens is higher than for $O_E$, and another weak maximum between 4 and 5 Å (with position depending on the cation) is noticeable. All these observations support the hypothesis that $O_C$ oxygen atoms tend to concentrate around the alkali ion.

In addition to RDFs, cumulative numbers $n_O(r)$ of O atoms found within a given distance $r$ from the $M^+$ ion are shown in Figure 3. From the plateaus of $n_O(r)$, we may conclude that the first coordination sphere is filled between 2 and 3 Å for $Li^+$ and $Na^+$ and between 3 and 4 Å for $K^+$. This justifies the choice of threshold distances used to calculate coordination numbers.

Only average coordination numbers are presented in Figure 3. To get more insight on how $M^+$–O interactions are related to the structure of the liquid at the molecular level, we calculated for each cation the number of coordinating caboxylate and ether oxygens ($CN(O_C)$ and $CN(O_E)$), the number of different anions providing these oxygen atoms ($NA(O_C)$ and $NA(O_E)$, respectively), and the $\Delta_{E-C}$ value: the number of coordinating ether oxygen atoms which belong to anions different from those providing carboxylate oxygens coordinating given metal ion. Values averaged over the last 50 ns of the trajectory and over all cations in the sample are collected with corresponding standard deviations in Table 2.

**Table 2. Parameters of the $M^+$ Coordination Averaged over the Last 50 ns of the MD Trajectory[a]**

| | $CN(O_C)^b$ | $CN(O_E)^b$ | $NA(O_C)^c$ | $NA(O_E)^c$ | $\Delta_{E-C}{}^d$ |
|---|---|---|---|---|---|
| Li | 3.5 ± 1.3 | 1.7 ± 1.4 | 3.0 ± 0.8 | 0.9 ± 0.6 | 0.5 ± 0.9 |
| Na | 4.1 ± 1.4 | 1.9 ± 1.5 | 3.6 ± 1.0 | 0.9 ± 0.6 | 0.2 ± 0.4 |
| K | 5.0 ± 1.7 | 2.4 ± 1.6 | 3.8 ± 1.0 | 1.1 ± 0.6 | 0.4 ± 0.5 |

[a]Standard deviations of calculated values are given as errors. [b]$CN(O_X)$ is the number of $O_X$ atoms coordinating the $M^+$ ion. [c]$NA(O_X)$ is the number of different $[TOTO]^-$ anions providing the coordinating $O_X$ atoms. [d]$\Delta_{E-C}$ is the number of coordinating $O_E$ atoms which belong to anions different from those providing $O_C$ atoms coordinating a given $M^+$ ion.

Despite the fact that average values become almost constant at the end of the trajectory, standard deviations are still quite large because values for individual ions may vary in a relatively broad range. Plots of the values obtained for each ion in a selected frame are shown in Figure S2 of the Supporting Information. If one reverses the problem and calculates the number of different $M^+$ cations coordinated to a given anion via $O_C$ or $O_E$ oxygens, these values will be exactly the same as $NA(O_C)$ and $NA(O_E)$.

Average $NA(O_E)$ values are smaller or only a little larger than 1, showing that in most cases all ether oxygen atoms coordinating the cation are from the same $[TOTO]^-$ anion. Mean $CN(O_C)$ values are larger than the average $NA(O_C)$ by about 0.5–1. Therefore, usually only one anion interacts with a given cation via both carboxylate oxygen atoms. Other $M^+$–$O_C$ interactions engage different anions; each of these anions provides only one $O_C$ atom to coordinate a given cation. The average $NA(O_C)$ is between 3 and 4; thus, each metal cation is coordinated to 3–4 $[TOTO]^-$; on the other hand, each anion has 3–4 metal ions within the distance of 3 or 4 Å from either carboxylate oxygen atom. Simultaneously, $\Delta_{E-C}$ values are small, meaning that only seldom does a $[TOTO]^-$ anion interact with $M^+$ solely via $O_E$ atoms without additional $M^+$–$O_C$ interactions. Sample plots of coordination sphere of selected $Na^+$ ions are presented in Figure S3 of the Supporting Information showing that indeed in the average situation there are groups of metal cations coordinated to carboxylate oxygens of neighboring anions.

Distributions of coordination numbers (i.e., probability of finding a given number of oxygen atoms within a specified distance from $M^+$) for all cations obtained from the last 10 ns of MD trajectories are displayed in Figure 4. With increasing radius of the ion (from Li to K), the maxima of CN histograms shift to higher values (average values increase in the same sequence as easily seen from Figures 2 and 4). The most probable number of all oxygen atoms around alkali cation is 5, 6, and 7 for $Li^+$, $Na^+$, and $K^+$, respectively. It is obvious that coordination by carboxylate oxygen atoms is favored: about 20–30% of $M^+$ ions is not coordinated to any ether oxygen ($CN(O_E) = 0$ in Figure 4), but there is always at least one carboxylate oxygen atom in the coordination sphere of the ion, and the coordination number for $O_C$ atoms reaches 7 and more. This leads to the conclusion that the metal ion is


dx.doi.org/10.1021/jp4070449 | J. Phys. Chem. B 2013, 117, 12583–12592

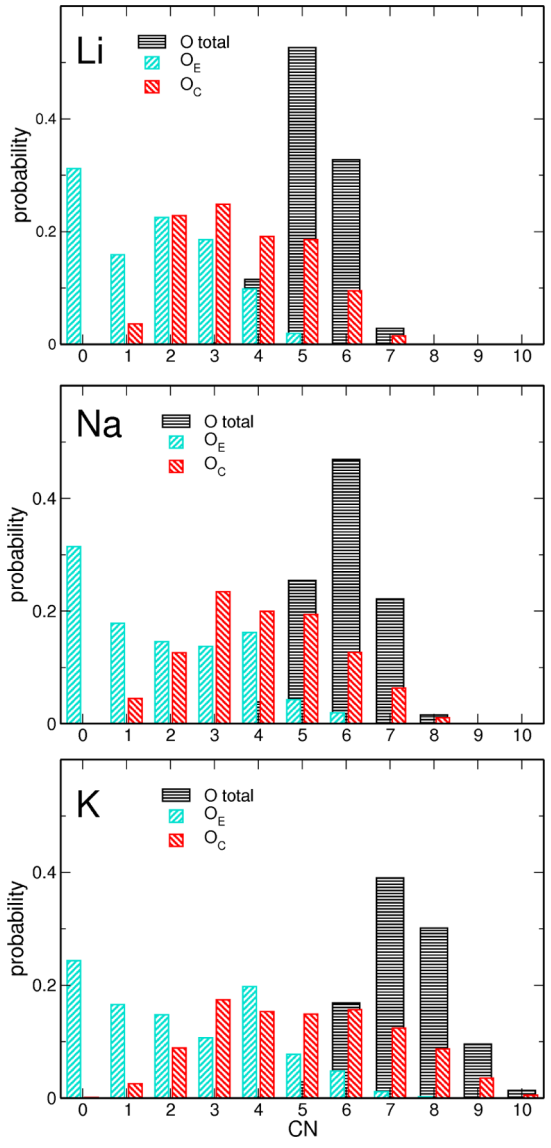


**Figure 4.** Distributions of $M^+$−O coordination numbers.

surrounded by at least four oxygen atoms from $[TOTO]^-$ anions with preference for carboxylate oxygens.

Results of similar analysis are presented in the Supporting Information for those structures I for which longer trajectories are available. Plots of radial distribution functions for structures I and III are practically indistinguishable. Slightly larger are the differences of CN and NA values, but again, the distributions of coordination numbers are almost the same. Therefore, we concluded that the $M^+$ coordination in both types of structures is the same.

All these data suggest that the cation−anion interactions lead to cross-linking in the structure of TOTO−M ionic liquids. Such cross-linking occurs mainly because of cation interactions with several anions via carboxylate oxygens. Cation−$O_E$ interactions are less important in this respect.

**3.3. Transport Properties.** Transport properties of the system, such as ion self-diffusion coefficients and conductivity, are related to ion movements and may be obtained using MD trajectories from mean square displacements (MSD) of ions. The cation and anion diffusion coefficients $D_i$ of ion $i$ were calculated from the slope of the time dependence of MSD:

$$D_i = \lim_{t\to\infty} \frac{1}{6t}\langle|\mathbf{R}_i(t) - \mathbf{R}_i(0)|^2\rangle \tag{2}$$

Of interest is also the collective ion diffusion coefficient

$$D_{\text{coll}} = \lim_{t\to\infty} \frac{1}{6tN}\sum_{i,j} z_i z_j\langle[\mathbf{R}_i(t) - \mathbf{R}_i(0)][\mathbf{R}_j(t) - \mathbf{R}_j(0)]\rangle \tag{3}$$

describing the mean square displacement of the charge when the correlations between ion movement are present. This quantity is related to the conductivity of the system, which can be expressed as[33]

$$\lambda = \lim_{t\to\infty} \frac{e^2}{6tVk_BT}\sum_{i,j} z_i z_j\langle[\mathbf{R}_i(t) - \mathbf{R}_i(0)]\,[\mathbf{R}_j(t) - \mathbf{R}_j(0)]\rangle \tag{4}$$

In the above formulas, $t$ stands for time, $N$ is the number of ions in the system, $V$ is the volume of the simulation box, $k_B$ is the Boltzmann's constant, $T$ is the temperature, $e$ is the elementary charge, $z_i$ and $z_j$ are the charges of ions $i$ and $j$, $\mathbf{R}_i(t)$ is the position of the $i$th ion at time $t$, and the brackets $\langle\rangle$ denote the ensemble average.

Collective ion diffusion coefficients $D_{\text{coll}}$ would reduce to average diffusion coefficients $D_{\text{avg}} = (D_{\text{cation}} + D_{\text{anion}})/2$ if there are no off-diagonal terms in eq 3, that is, in the case when the correlations between movements of different ions are negligible.

Plots of MSD for different ions are displayed in Figure 5. The MSD scales with time as MSD $\propto t^{\beta}$ and for diffusive motion $\beta = 1$ (thus the plot of MSD vs $t$ is a straight line). This regime is achieved for long-time scale, and for intermediate time scales,

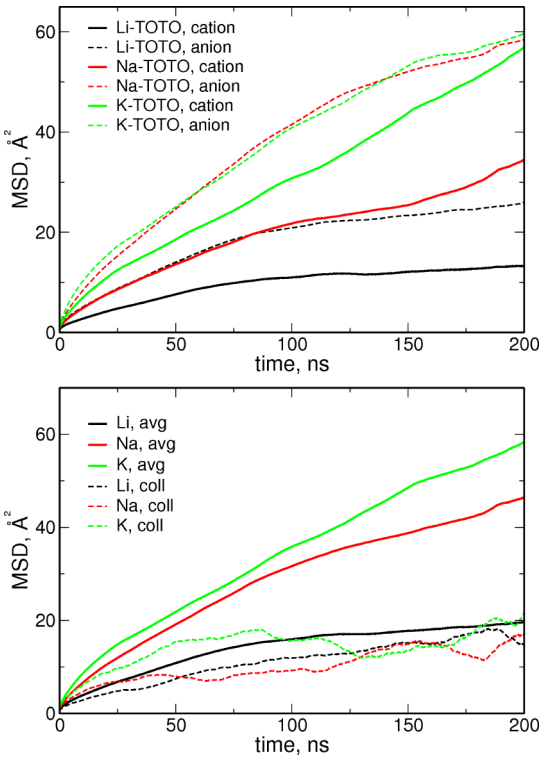


**Figure 5.** Mean square displacements (upper panel) and collective and average mean square displacements (lower panel) of ions.


dx.doi.org/10.1021/jp4070449 | J. Phys. Chem. B 2013, 117, 12583−12592

behavior of the system is subdiffusive with $\beta < 1$. Unfortunately, with large viscosity of TOTO-based liquids and slow dynamics, extremely long times are needed to reach the ideal diffusive behavior even at high temperature. It is apparent from Figure 5 that the MSD plots are nonlinear; therefore, estimates of diffusion coefficients should be taken with care. In the diffusive regime, the plot of log(MSD) versus log($t$) is a straight line with the slope $\beta = 1$. Glasslike behavior is indicated by smaller $\beta$ values. Double-logarithmic plots of MSD for cations and anions as a function of time are shown as insets in Figure 6. Only in

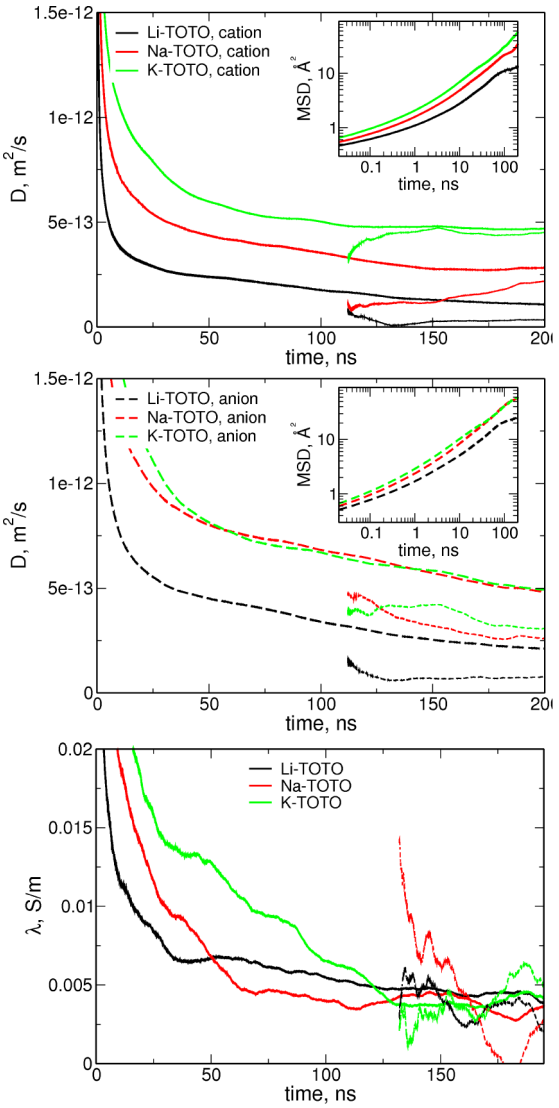


**Figure 6.** Diffusion coefficients (upper and middle panels) and conductivity (bottom panel) calculated for increased time intervals. Thin lines: data computed for a part of the trajectory, shifted in the time scale to the starting point. Insets: double-log plots of mean square displacements of ions.

the case of $K^+$ movements in the K−TOTO liquid does the slope of the line approach one; for other ions, it is smaller but is increasing. Most systems are, therefore, still in the subdiffusive regime.

To find some estimates of diffusion coefficients, we used the data shown in Figure 5 to calculate $D(t) = \Delta\text{MSD}/\Delta t$ using increasing time intervals. The results are shown in Figure 6. $D(t)$ decreases rapidly for small $t$; for long times, the curves tend to stabilize especially for cations. It has been observed in MD simulations for ionic liquids that $D(t)$ stabilizes before true self-diffusive regime with $\beta = 1$ is reached.[34] Values approached by $D(t)$ at the end of the time interval have been taken as the estimates of diffusion coefficients. Another set of data (thin lines in Figure 6) is obtained when only about a half of the trajectory from Figure 5 is used to calculate $D(t)$ (time scale for these data is shifted to the starting point). For linearly increasing MSD, this would yield a horizontal line at the same $D$ value as obtained for full time interval; deviations appear for nonlinearly increasing MSD. We therefore used the difference between these two values as an error estimate of the diffusion coefficient. As readily seen, the smallest error is observed for movements of $K^+$ cation for which the MSD versus time dependence is closest to linear.

Diffusion coefficients for $M^+$ and $[TOTO]^-$ calculated for the last 200 ns of MD trajectories are collected in Table 3.

**Table 3. Diffusion Coefficients for Cations and Anions Calculated from MD Simulations for $M^+$−TOTO Ionic Liquids**

| cation | $D_+$ [$10^{-13}$ m$^2$/s] | $D_-$ [$10^{-13}$ m$^2$/s] |
|---|---|---|
| $Li^+$ | 1.1 ± 0.8 | 2.1 ± 1.2 |
| $Na^+$ | 2.9 ± 0.7 | 4.9 ± 2.1 |
| $K^+$ | 4.7 ± 0.3 | 5.0 ± 1.8 |

Results for structures of type I are presented in the Supporting Information. Obtained $D$ values are smaller for systems I (which were constructed in such a way that the cations were initially complexed to carboxylate oxygens and therefore were more strongly bound); nevertheless, they agree with the data for structures III within estimated error bars.

Diffusion coefficients for cations increase from $Li^+$ to $K^+$, that is, in the order of decreasing strength of $M^+$−$[TOTO]^-$ interactions as calculated in section 2. Because of the cross-linking (strongest for $Li^+$) occurring in the liquid structure, which restricts also the movements of anions, the diffusion coefficient for $[TOTO]^-$ increases in the same sequence of cations. In the Li−TOTO liquid, anion diffusion is the slowest in agreement with experimental observation of very high viscosity of this system.[4] Our results support the conclusion of ref 5 that this is an effect of cation linkers between TOTO anions. $D_M$ values are smaller than $D_{TOTO}$ which may be rationalized by the structure of the system in which most cations are located in the aggregates stabilized by interactions with carboxylate oxygens. Interactions in such aggregates reduce the probability of cation escape; moreover, any free cations are likely to be trapped at these sites.

MSD values for correlated ion movements and the average diffusion coefficients $D_{avg}$ are displayed in Figure 5, and the analysis similar to that performed to estimate the errors of diffusion coefficients is shown in the bottom panel of Figure 6. $D_{avg}$ increases from TOTO−Li to TOTO−K as a consequence of increasing diffusion coefficients for individual ions. However, collective ion movements are the same for all cations within the accuracy of simulations. This behavior originates in increasing amount of off-diagonal correlations reducing $D_{coll}$. In Figure 7, $D_{coll}$ is separated into contributions arising from different ion−ion correlations. Off-diagonal cation−anion contributions are positive (cation−anion movements are anticorrelated); therefore, they increase the conductivity. On the other hand, off-diagonal anion−anion term has a negative sign and contributes


dx.doi.org/10.1021/jp4070449 | J. Phys. Chem. B 2013, 117, 12583−12592

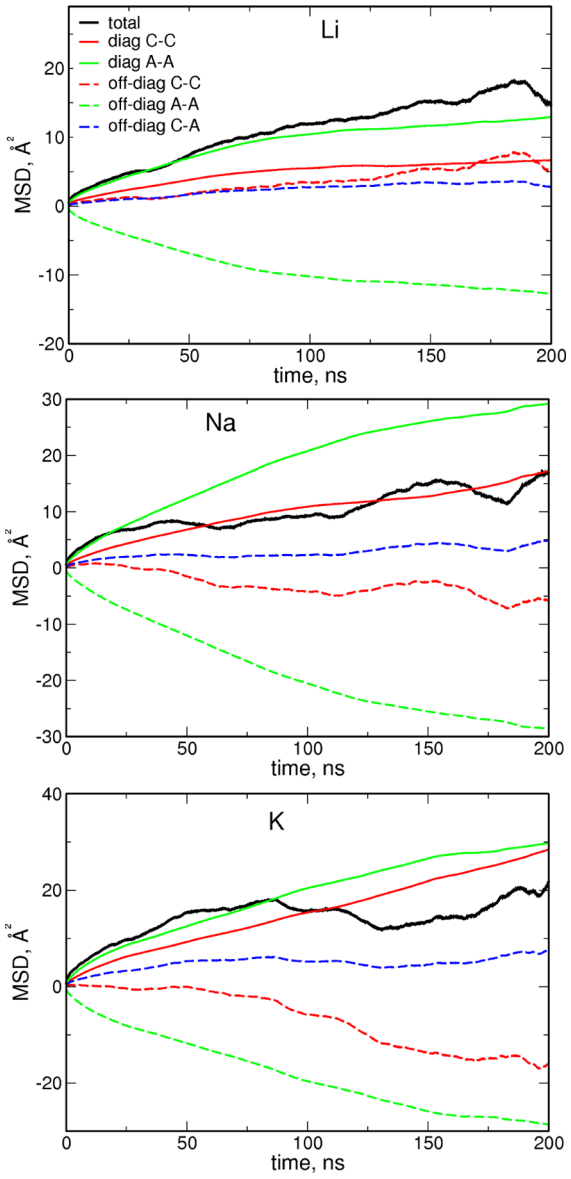


**Figure 7.** Diagonal and off-diagonal contributions to the total collective mean square displacement of ions in M−TOTO.

to the decrease of $D_{coll}$. Off-diagonal cation−cation contribution changes from a slightly positive value for $Li^+$ to a negative value for $Na^+$ and $K^+$. We can see that the reduction of $D_{coll}$ with respect to $D_{avg}$ is due to anticorrelated motions of ions of the same charge. These results are consistent with findings of a model study,[35] comparing charge transport in ionic liquids and electrolyte solutions. It has been shown that in molten salts and ionic liquids anticorrelated motion of ions of opposite charge increases the overall conductivity. Conversely, anticorrelated motions of ions of the same charge (anion−anion and cation−cation) yield negative contribution to the collective diffusion coefficient therefore leading to conductivity decrease.[35] Our MD results exhibit all these features with the exception of correlated cation motions in Li−TOTO. We may rationalize this behavior taking into account that $Li^+$ ions tend to form clusters of several cations (glued by counterions), and therefore, their motions are likely to be correlated. This is supported by the fact that for Na−TOTO for which interionic interactions are weaker, cation−cation motions become anticorrelated, and this feature is even more pronounced for K−TOTO with the weakest interactions.

As the result of similar $D_{coll}$ values, calculated conductivity is practically the same for all three systems and does not depend on the alkali cation. From the data presented in Figure 6, it was estimated as $(4 \pm 2) \times 10^{-3}$ S/m. The experimental value for $Na^+$−$[TOTO]^-$ is $2.4 \times 10^{-2}$ S/m (ref 4); therefore, MD simulations underestimated the conductivity about 6 times. This is not surprising because of deficiencies of nonpolarizable force-field parametrization. Taking this into account, as well as the difficulties with simulations for systems with very low diffusivity, we conclude that our result agrees reasonably well with measured conductivity. It has been shown for similar systems (poly(ethylene oxide)-based electrolytes) that accounting for polarization effects through polarizable force-field increases diffusion coefficients and conductivity by an order of magnitude.[22] Similar effects have been observed also in several MD simulations of ionic liquids.[36−38] Increase of diffusivity in polarizable simulations is therefore a rather general feature (which may be attributed to the reduction of cage effect[36]), and such dependence may be expected also for M−TOTO systems. Applying a polarizable force-field (unfortunately computationally expensive) would presumably increase calculated conductivity, improving agreement with the experiment.

## 4. CONCLUSIONS

We have performed classical molecular dynamics simulations of ionic liquids based on $[TOTO]^-$ anions and alkali metal cations supplemented by quantum-chemical calculations. Optimized geometries of 1:1 cation−anion complexes and calculated binding energies show that cations have significantly larger affinity to carboxylate oxygen atoms than to ether oxygens. Interaction strength of $[TOTO]^-$ with cations decreases in the order Li > Na > K.

Analysis of cation coordination zones in the MD trajectories indicates that preferable coordination of the cation is to carboxylate oxygen atoms from $[TOTO]^-$. Typically, about four to six oxygen atoms from several different anions are involved in interactions. Additional stabilization is provided by interactions with ether oxygens; nevertheless, the percentage of cations complexed almost exclusively by ether oxygens in a crown-ether-like fashion is small. Metal ions tend to aggregate in regions occupied by $COO^-$ ends of anions; in this way, $M^+$−$O_C$ interactions create cross-links in the liquid. Metal−ether oxygen interactions also contribute to linking but in a much smaller proportion.

As a result of networking, diffusion of ions in the liquid is suppressed. Diffusion coefficients increase in the order of decreasing ion−ion interactions, that is, from Li−TOTO to K−TOTO. Conductivity of the Na−TOTO system calculated at 400 K is about 6 times lower than experimentally determined; the difference may be partially attributed to the use of nonpolarizable force field.

Complexation energies and MD simulated structures support the suggestion presented in the experimental study[5] that in Na−TOTO most cations are involved in interactions with carboxylate groups and cation interactions with oxygen atoms from different TOTO moieties create links in the liquid. Likewise, the small mobility of $[TOTO]^-$ anions obtained for the system with $Li^+$ agrees with the explanation suggested in ref 5 that large viscosity observed for Li−TOTO is due to strong cross-linking.


dx.doi.org/10.1021/jp4070449 | J. Phys. Chem. B 2013, 117, 12583−12592

The main difference between our data and the picture suggested in ref 5 is that we predict a more important role of cation−carboxylate oxygen interactions. Instead of a liquid composed mainly of 1:1 cation−anion complexes networked by additional cation−ether oxygen interactions as postulated in ref 5, MD simulations yield structures where multiple cations and multiple $COO^-$ groups (from different anions) concentrate in some regions, creating strong links between $[TOTO]^-$ anions. The difference is therefore rather not in general conclusions about cross-linked structure but in the relative importance of different factors responsible for stabilization of this structure.

Analysis of different contributions to the electric conductivity shows that correlations between ion movements are of great importance for M−TOTO liquids. Anticorrelated motions of ions of the same charge reduce significantly the conductivity of ionic liquid, while anion−cation anticorrelations lead to its increase in agreement with the results of model analysis of charge transport.[35]

The presented results of theoretical modeling of M−TOTO ionic liquids are in agreement with available experimental data and, offering insight into intermolecular interactions at the microscopic level, help to better understand the relationship between M−TOTO structure and its physicochemical properties.

## ■ ASSOCIATED CONTENT

### Supporting Information

Partial atomic charges used in FF calculations, comparison of quantum-chemical and FF complexation energies, benchmarks for GP GPU calculations, plots of average end-to-end distance in MD simulations, coordination data for selected systems, analysis of the MD data for structures of type I. This material is available free of charge via the Internet at http://pubs.acs.org.

## ■ AUTHOR INFORMATION

### Corresponding Author

*Fax: +48 12 6340515, e-mail: eilmes@chemia.uj.edu.pl.

### Notes

The authors declare no competing financial interest.

## ■ ACKNOWLEDGMENTS

The equipment used in Gaussian 09 calculations was purchased with the financial support from the European Regional Development Fund in the framework of the Polish Innovation Economy Operational Program (contract no. POIG.02.01.00-12-023/08). GP GPU calculations were carried out with the support of the "HPC Infrastructure for Grand Challenges of Science and Engineering" Project cofinanced with the above bodies. This research was supported in part by PL-Grid Infrastructure.

## ■ REFERENCES

(1) Welton, T. Room-Temperature Ionic Liquids. Solvents for Synthesis and Catalysis. *Chem. Rev.* **1999**, *99*, 2071−2083.

(2) Wasserscheid, P.; Keim, W. Ionic Liquids − New Solutions for Transition Metal Catalysis. *Angew. Chem., Int. Ed.* **2000**, *39*, 3772−3789.

(3) Petkovic, M.; Seddon, K. R.; Rebelo, L. P. N.; Silva Pereira, C. Ionic Liquids: A Pathway to Environmental Acceptability. *Chem. Soc. Rev.* **2011**, *40*, 1383−1403.

(4) Zech, O.; Kellermeier, M.; Thomaier, S.; Maurer, E.; Klein, R.; Schreiner, Ch.; Kunz, W. Alkali Metal Oligoether Carboxylates − A New Class of Ionic Liquids. *Chem.—Eur. J.* **2009**, *15*, 1341−1345.

(5) Zech, O.; Hunger, J.; Sangoro, J. R.; Iacob, C.; Kremer, F.; Kunz, W.; Buchner, R. Correlation Between Polarity Parameters and Dielectric Properties of [Na][TOTO] − A Sodium Ionic Liquid. *Phys. Chem. Chem. Phys.* **2010**, *12*, 14341−14350.

(6) Klein, R.; Zech, O.; Maurer, E.; Kellermeier, M.; Kunz, W. Oligoether Carboxylates: Task-Specific Room-Temperature Ionic Liquids. *J. Phys. Chem. B* **2011**, *115*, 8961−8969.

(7) Daschakraborty, S.; Biswas, R. Stokes Shift Dynamics of [Na][TOTO] − A New Class of Ionic Liquids: A Comparative Study with More Common Imidazolium Analogs. *Chem. Phys. Lett.* **2012**, *545*, 54−59.

(8) Maginn, E. J. Atomistic Simulation of the Thermodynamic and Transport Properties of Ionic Liquids. *Acc. Chem. Res.* **2007**, *40*, 1200−1207.

(9) Bhargava, B. L.; Balasubramanian, S.; Klein, M. L. Modelling Room Temperature Ionic Liquids. *Chem. Commun.* **2008**, 3339−3351.

(10) Kirchner, B. Ionic Liquids from Theoretical Investigations. *Top. Curr. Chem.* **2009**, *290*, 213−262.

(11) Sambasivarao, S. V.; Acevedo, O. Development of OPLS-AA Force Field Parameters for 68 Unique Ionic Liquids. *J. Chem. Theory Comput.* **2009**, *5*, 1038−1050.

(12) Maginn, E. J. Molecular Simulation of Ionic Liquids: Current Status and Future Opportunities. *J. Phys.: Condens. Matter* **2009**, *21*, 373101/1−373101/17.

(13) Izgorodina, E. I. Towards Large-Scale, Fully *Ab Initio* Calculations of Ionic Liquids. *Phys. Chem. Chem. Phys.* **2011**, *13*, 4189−4207.

(14) Dommert, F.; Wendler, K.; Berger, R.; Delle Site, L.; Holm, C. Force Fields for Studying the Structure and Dynamics of Ionic Liquids: A Critical Review of Recent Developments. *ChemPhysChem* **2012**, *13*, 1625−1637.

(15) Johansson, P.; Gejji, S. P.; Tegenfeldt, J.; Lindgren, J. Local Coordination and Conformation in Polyether Electrolytes: Geometries of *M*-Triglyme Complexes (*M* = Li, Na, K, Mg and Ca) from Ab-Initio Molecular Orbital Calculations. *Solid State Ionics* **1996**, *86−88*, 297−302.

(16) Sutjianto, A.; Curtiss, L. A. $Li^+$ - Diglyme Complexes: Barriers to Lithium Cation Migration. *J. Phys. Chem. A* **1998**, *102*, 968−974.

(17) Johansson, P.; Tegenfeldt, J.; Lindgren, J. Modeling Amorphous Lithium Salt-PEO Polymer Electrolytes: Ab Initio Calculations of Lithium Ion-Tetra-, Penta- and Hexaglyme Complexes. *Polymer* **1999**, *40*, 4399−4406.

(18) Baboul, A. G.; Redfern, P. C.; Sutjianto, A.; Curtiss, L. A. $Li^+$-$(Diglyme)_2$ and $LiClO_4$-Diglyme Complexes: Barriers to Lithium Ion Migration. *J. Am. Chem. Soc.* **1999**, *121*, 7220−7227.

(19) Redfern, P. C.; Curtiss, L. A. Quantum Chemical Studies of $Li^+$ Cation Binding to Polyalkyloxides. *J. Power Sources* **2002**, *110*, 401−405.

(20) Eilmes, A.; Kubisiak, P. Polarizable Continuum Model Study on the Solvent Effect of Polymer Matrix in Poly(ethylene oxide)-Based Solid Electrolyte. *J. Phys. Chem. A* **2008**, *112*, 8849−8857.

(21) Halley, J. W.; Duan, Y.; Curtiss, L. A.; Baboul, A. G. Lithium Perchlorate Ion Pairing in a Model of Amorphous Polyethylene Oxide. *J. Chem. Phys.* **1999**, *111*, 3302−3308.

(22) Borodin, O.; Smith, G. D.; Douglas, R. Force Field Development and MD Simulations of Poly(ethylene oxide)/$LiBF_4$ Polymer Electrolytes. *J. Phys. Chem. B* **2003**, *107*, 6824−6837.

(23) Siqueira, L. J. A.; Ribeiro, M. C. C. Molecular Dynamics Simulation of the Polymer Electrolyte Poly(ethylene oxide)/$LiClO_4$. I. Structural Properties. *J. Chem. Phys.* **2005**, *122*, 194911/1−194911/8.

(24) Siqueira, L. J. A.; Ribeiro, M. C. C. Molecular Dynamics Simulation of the Polymer Electrolyte Poly(ethylene oxide)/$LiClO_4$. II. Dynamical Properties. *J. Chem. Phys.* **2006**, *125*, 214903/1−214903/8.

(25) Borodin, O.; Smith, G. D. Development of Many-Body Polarizable Force Fields for Li-Battery Applications: 2. LiTFSI-Doped Oligoether, Polyether, and Carbonate-Based Electrolytes. *J. Phys. Chem. B* **2006**, *110*, 6293−6299.

(26) Eilmes, A.; Kubisiak, P. Molecular Dynamics Study on the Effect of Lewis Acid Centers in Poly(ethylene oxide)/$LiClO_4$ Polymer Electrolyte. *J. Phys. Chem. B* **2011**, *115*, 14938−14946.
(27) Frisch, M. J.; Trucks, G. W.; Schlegel, H. B.; Scuseria, G. E.; Robb, M. A.; Cheeseman, J. R.; Scalmani, G.; Barone, V.; Mennucci, B.; Petersson, G. A. et al. *Gaussian 09* , revision A.02; Gaussian, Inc.: Wallingford, CT, 2009.
(28) Jorgensen, W. L.; Maxwell, D. S.; Tirado-Rives, J. Development and Testing of the OPLS All-Atom Force Field on Conformational Energetics and Properties of Organic Liquids. *J. Am. Chem. Soc.* **1996**, *118*, 11225−11236.
(29) Jensen, K. P.; Jorgensen, W. L. Halide, Ammonium, and Alkali Metal Ion Parameters for Modeling Aqueous Solutions. *J. Chem. Theory Comput.* **2006**, *2*, 1499−1509.
(30) Phillips, J. C.; Braun, R.; Wang, W.; Gumbart, J.; Tajkhorshid, E.; Villa, E.; Chipot, Ch.; Skeel, R. D.; Kalé, L.; Schulten, K. Scalable Molecular Dynamics with NAMD. *J. Comput. Chem.* **2005**, *26*, 1781−1802.
(31) Martinez, L.; Andrade, R.; Birgin, E. G.; Martinez, J. M. PACKMOL: A Package for Building Initial Configurations for Molecular Dynamics Simulations. *J. Comput. Chem.* **2009**, *30*, 2157−2164.
(32) Zech, O. Ionic Liquids in Microemulsions − a Concept to Extend the Conventional Thermal Stability Range of Microemulsions. PhD Dissertation, Universität Regensburg, 2010; http://epub.uni-regensburg.de/12217/.
(33) Müller-Plathe, F. Permeation of Polymers − A Computational Approach. *Acta Polym.* **1994**, *45*, 259−293.
(34) Cadena, C.; Zhao, Q.; Snurr, R. Q.; Maginn, E. J. Molecular Modeling and Experimental Studies of the Thermodynamic and Transport Properties of Pyridinium-Based Ionic Liquids. *J. Phys. Chem. B* **2006**, *110*, 2821−2832.
(35) Kashyap, H. K.; Annapureddy, H. V. R.; Raineri, F. O.; Margulis, C. J. How Is Charge Transport Different in Ionic Liquids and Electrolyte Solutions? *J. Phys. Chem. B* **2011**, *115*, 13212−13221.
(36) Yan, T.; Burnham, Ch. J.; Del Pópolo, M. G.; Voth, G. A. Molecular Dynamics Simulation of Ionic Liquids: The Effect of Electronic Polarizability. *J. Phys. Chem. B* **2004**, *108*, 11877−11881.
(37) Borodin, O. Polarizable Force Field Development and Molecular Dynamics Simulations of Ionic Liquids. *J. Phys. Chem. B* **2009**, *113*, 11463−11478.
(38) Schröder, Ch. Comparing Reduced Partial Charge Models with Polarizable Simulations of Ionic Liquids. *Phys. Chem. Chem. Phys.* **2012**, *14*, 3089−3102.